Thermal cycling and degradation mechanisms of compressive mica-based seals for solid oxide fuel cells

Yeong-shyung Chou[*], Jeffry W. Stevenson

Materials Resource Department, Pacific Northwest National Laboratories, P.O. Box 999, Richland, WA 99352, USA

Abstract

Thermal cycling was conducted on compressive mica seals at 800 °C in air. Thin (~0.1 mm) Muscovite mica was pressed between a metal pipe and an alumina substrate and tested for leak rates at a stress of 100 psi in the plain (mica only) and the hybrid design. The hybrid design involves adding two glass interlayers and was found to greatly reduce the leak rates in an earlier paper. Two metals (Inconel #600 and SS430) with high and low coefficients of thermal expansion (CTE) were used to evaluate the effect of CTE mismatch on thermal cycling. The results showed that the leak rates were lower for the hybrid design than the plain micas. In addition, using the lower CTE (SS430) metal pipe resulted in lower leak rates as compared to Inconel #600 metal (high CTE). In general, the leak rates increased with the number of thermal cycles; however, it tended to level off after several tens of thermal cycles. Microstructure examination using scanning electron microscopy revealed steps, indents, fragmentation and particle formation on the mica after thermal cycling. CTE measurement of the heat-treated Muscovite mica showed a relatively low value of ~7 ppm/°C. The cause for the degradation of the mica is discussed.
© 2002 Elsevier Science B.V. All rights reserved.

Keywords: Thermal cycling; Compressive mica-based seals; Solid oxide fuel cells

1. Introduction

Planar solid oxide fuel cells (SOFCs) are believed to potentially offer lower cost and higher power density per unit volume compared to tubular designs [1–4]. The planar SOFC designs, however, face many challenges in materials development, processing, and system integration that must be overcome. One of these challenges is the seal technology. The seal needs to provide sufficiently low leak rates that leaks (e.g. H_2 into the air stream) will not cause undesirable local heating which can lead to the structural or functional failure of the stack. The seal also needs to have long-term stability and cause no degradation of the materials with which they are in contact (e.g. stabilized zirconia, interconnect, and electrodes) at the elevated temperatures (e.g. 800 °C) and harsh environments (oxidizing, reducing, and humid) typical of SOFCs during operation. Finally, the seal has to survive many thermal cycles during routine operations; this appears to be the most challenging part of the seal development.

So far, most SOFC seal development has focused on glass or glass–ceramic seals although other approaches, such as cement seals, mica glass–ceramics, brazes, and compressive seals have been proposed [5–9]. None of the previous studies investigated the issue of thermal cycling that is very critical for materials have different coefficients of thermal expansion (CTE), especially for SOFCs with metallic interconnects. In SOFCs, the CTE of the electrolyte (8YSZ) is about 11 ppm/°C, the Ni-YSZ anode is about 12.5, and that of the metallic interconnect can be unfavorably higher. Mismatches in CTE can result in undesirable residual stresses upon cooling, which can lead to structural failure. As a result, the candidates for metallic interconnects for glass sealed stacks become rather limited. The CTE mismatch between the YSZ electrolyte and the metallic interconnect can be minimized by using Ni-YSZ anode-supported electrolytes instead of thick electrolyte-supported cells and a ferritic steel, such as SS430. But, the use of glass seals in this combination can still face problems due to the formation of undesirable phases, such as $m\text{-}ZrO_2$, cordierite (CTE $\approx$ 2 ppm/°C), and cristobolite [10]. On the other hand, if the cell and the metallic interconnect are not rigidly bonded with each other (as in the case of compressive seals), residual stresses should be eliminated or at least substantially reduced.

---

[*] Corresponding author. Tel.: +1-509-375-2527; fax: +1-509-375-2186.
E-mail address: yeong-shyung.chou@pnl.gov (Y.-s. Chou).

By eliminating the need for closely matching CTE, compressive seals may expand the list of candidate interconnect materials, whether ceramic or metallic. The research in the area of compressive seals for SOFCs is still in its early stages and very little data is available. Simner and Stevenson [9] studied compressive mica seals for SOFC applications. They found that cleaved natural Muscovite mica sheets performed better than mica papers. High temperature leak rates of about 0.33–0.65 sccm/cm were reported on small test coupons. Recently, the present authors developed a hybrid compressive mica seal and reported a very low leak rate of $\sim 1.6 \times 10^{-4}$ sccm/cm at the same conditions [11]. In the present paper, we report results from a study of the effects of thermal cycling on the properties of the hybrid compressive mica seal. Results of leak rates of single layer mica seals as well as multi-layer mica seals are reported, and the degradation of performance due to thermal cycling is discussed.

2. Experimental

2.1. Raw materials and characterization

The mica investigated in this study is a natural cleaved single crystal Muscovite mica ($KAl_2(AlSi_3O_{10})(F,OH)_2$) in the form of thin sheet ($\sim 100\ \mu m$ thick). The cleaved Muscovite single crystal sheet is transparent as received and becomes opaque after losing chemical water at elevated temperatures [9]. The cleaved single crystal micas were found to have much lower leak rates as compared to other types of mica (such as mica "paper," which is composed of discrete mica flakes bonded together with organic binders) and were therefore selected for this study [9,11]. For the hybrid compressive seal tests, a borosilicate glass filter paper was used as the compliant interlayers. The linear thermal expansion of the Muscovite mica was also measured by dilatometry from room temperature to 800 °C in air. Two arbitrary orthogonal directions along the basal planes were tested. The Muscovite micas were first heat-treated at 850 °C for 6 h before laying 10 layers together for CTE measurement. The average (RT to 800 °C) CTE along two arbitrary orthogonal directions were found to be 6.88 and 6.91 ppm/°C, suggesting they are isotropic along the basal plane. The CTE perpendicular to the basal plane was reported to be ~ 14 ppm/°C (RT to ~ 600 °C) [12]. The high CTE is likely due to the chemical waters were still in the structure at the testing temperature.

Degradation characterization of the seals was conducted after the thermal cycle tests using scanning electron microscopy as well as optical microscopy.

2.2. Leak tests

Mica samples were cut into ~ 1.5 in. squares with a 0.5 in. diameter central hole. The mica squares were then pressed
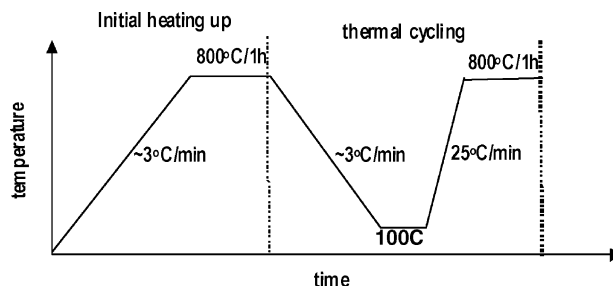

Fig. 1. Temperature profile for thermal cycling.

between a metal pipe (Inconel #600 or SS430) and a dense alumina substrate. For hybrid compressive seals, a glass interlayer was placed between the metal pipe/mica interface and the mica/alumina interface. The glass contains $\sim 58\%$ SiO_2, $\sim 9\%$ B_2O_3, $\sim 11\%$ Na_2O, $\sim 6\%$ Al_2O_3, $\sim 4\%$ BaO, and ZnO, CaO and K_2O. Samples were heated in a clamshell furnace at a heating rate about ~ 3 °C/min to 800 °C in the first heating run. In the following thermal cycles, it was heated at a faster rate of ~ 25 °C/min to 800 °C to simulate a rapid system start-up. The thermal cycling was conducted between 100 and 800 °C in air. The heating and cooling profiles are shown in Fig. 1. A compressive load was applied continuously using a universal mechanical tester with a constant load control (Model 5581, Instron, Canton, MA). The details of the experimental setup and the calculation of the normalized leak rates (in standard cubic centimeter per minute per unit length of seal, i.e. sccm/cm) were given in an earlier paper [11]. For multiple layer tests, two metal spacers were investigated: SS430 and SS304. The former has a lower coefficient of thermal expansion (CTE) (about 12.5 ppm/°C) than the latter (~ 19 ppm/°C). Ring type metal discs were cut from a large metal sheet (~ 0.010 in. thick) and flattened under a compressive load at ~ 700 °C. For multi-layer testing, the test specimen consisted of six mica layers, five metal rings and 12 glass interlayers as shown schematically in Fig. 2.
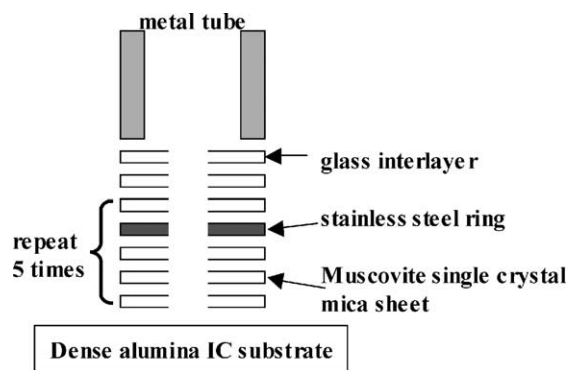

Fig. 2. Schematic diagram of the assembly for multi-layer thermal cycling test. There are six layers of mica, five layers of metal ring spacer, and 12 layers of glass.

3. Results and discussion

3.1. Choice of metal pipe for loading

Metallic interconnects are considered to be the leading candidates (compared to ceramic interconnects, such as lanthanum chromite) for planar stacks operating at temperatures below 800 °C. For compressive seals, the list of candidate interconnect alloys should be broadened since the interconnect is not rigidly bonded with the PEN (positive electrode–electrolyte–negative electrode) ceramic part, as compared to the glass seals. To test the compressive seals, two high temperature alloys were selected as the loading metal pipes: Inconel #600 and SS430. The former has higher strength, more oxidation resistance, and a higher CTE (∼19 ppm/°C) compared to the latter (CTE of ∼12.5 ppm/°C, which is close to that of anode-supported cells).

3.2. Effect of thermal cycling on the leak rates of single layer mica in plain (without glass) design

The 800 °C leak rates for the Muscovite single crystal micas are summarized in Table 1 for the plain design (without glass interlayers) as well as the hybrid design (with glass interlayers). The normalized leak rates are also plotted as a function of the thermal cycles for the plain design in Fig. 3. The leak rates showed an abrupt increase in the first couple of cycles. For example, the normalized leak rate was
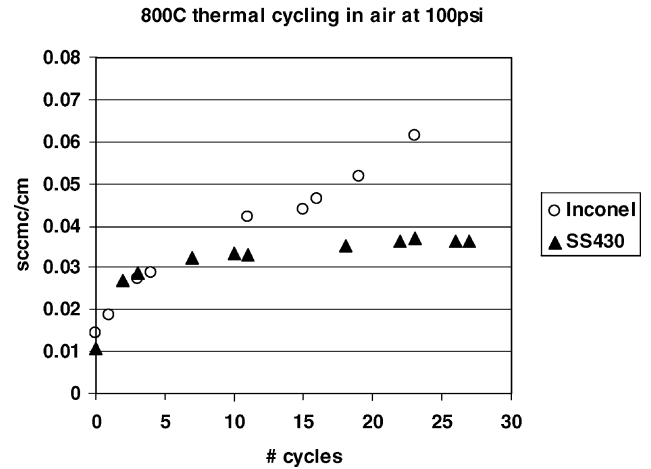

Fig. 3. Effect of thermal cycling on the normalized leak rates for a single layer (∼0.1 mm thick) Muscovite single crystal mica in plain design (without the glass interlayers) at 800 °C and a compressive stress of 100 psi in air.

∼0.011 sccm/cm before the test, and it was ∼0.027 sccm/cm after just 2 thermal cycles for SS430 metal. Similar behavior was observed for Inconel #600. However, the leak rates tended to level off after ∼10 cycles for the SS430, while they continued to increase for Inconel #600. The leak increase per thermal cycle for SS430 (in the last ∼10 cycles) was only ∼ 1.4×10^{-4} sccm/cm per cycle, while it was about 11 times higher for Inconel #600 (∼ 1.6×10^{-3} sccm/cm per cycle). The much higher leak rate increase per cycle is likely due to the large CTE mismatch for the Inconel #600-mica pair (ΔCTE $\cong$ 12 ppm/°C) compared to that of the SS430-mica pair (ΔCTE $\cong$ 5.5 ppm/°C). As observed in an earlier paper, the major leaks for compressive mica seals occur through the interfaces, i.e. metal to mica and/or mica to alumina substrate, rather than through the sublayers of the mica itself [11]. The present results clearly suggest that the major leak in the plain design is from the metal-to-mica interface rather than the mica-to-alumina substrate interface. This is consistent with the fact that the CTE mismatch between mica and alumina is even smaller (ΔCTE $\cong$ 2 ppm/°C).

3.3. Effect of thermal cycling on the leak rates of single layer mica in hybrid (with glass) design

Fig. 4 shows the effect of thermal cycling on the normalized leak rates of the Muscovite mica in the hybrid design, i.e., with the glass interlayers inserted at the metal–mica and mica–alumina interfaces (Fig. 2). A similar trend was observed in that there is an abrupt increase in the leak rates during the first couple of thermal cycles. The abrupt increase is more distinct for the micas in the hybrid design since the leak rates before the thermal cycle test were much lower (∼2–6 × 10^{-4} sccm/cm). It is also evident that the larger the CTE mismatch between mica and the metal pipe, the higher the leak rate, and the higher the leak rate increase per
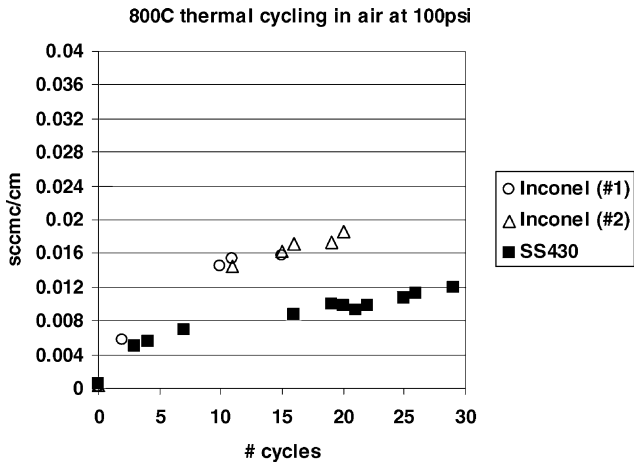
Table 1
Normalized leak rates (sccm/cm) of a single layer Muscovite single crystal mica in plain and hybrid design

Number of cycles	Plain		Hybrid		
	Inconel	SS430	Inconel #1	Inconel #2	SS430
0	0.0142	0.0106	0.00016	0.0003	0.00055
1	0.0185				
2		0.0268	0.0058		
3	0.0272	0.0287			0.00502
4	0.0287				0.00559
7		0.0323			0.00689
10		0.0334	0.0145		
11	0.0418	0.0330	0.0153	0.0145	
14					
15	0.0436		0.0157	0.0162	
16	0.0462			0.0172	0.0088
18		0.0351			
19	0.0518			0.0173	0.01
20				0.0185	0.0099
21					0.0092
22		0.0361			0.0099
23	0.0614	0.0368			
25					0.0107
26		0.0361			0.0112
27		0.0364			
29					0.0119

Thermally cycled in air at 800 °C and 100 psi. Two metal pipes (SS430 and Inconel #600) were tested.

Fig. 4. Effect of thermal cycling on the normalized leak rates for a single layer (∼0.1 mm thick) Muscovite single crystal mica in the hybrid design (with the glass interlayers) at 800 °C and a compressive stress of 100 psi in air.

Table 2
Normalized leak rates (sccm/cm) for the multilayer assemblies during 800 °C thermal cycling under a load of 50 lbs

Number of cycles	SS430	SS304
0	0.0087	0.0051
1	0.0114	0.0085
2	0.0135	
3	0.0129	
4		0.0142
7	0.0181	
8		0.0195
12		0.0233
13		0.0214
17		0.0272
20		0.0281
40		0.0413

Note the leak rates were normalized with respect to the outer leak length (10.5 cm) and to a gas pressure gradient of 2 psi across the six layers of mica.

thermal cycle. For example, the normalized leak rate increase per thermal cycle was ∼4.4×10^{-4} sccm/cm per cycle for Inconel #600, and it was ∼1.9×10^{-4} sccm/cm per cycle for SS430 (using the data of approximately the last 10 cycles in Fig. 4). For SS430, the leak rate change per thermal cycle was similar for both the plain and the hybrid design, while, for the Inconel #600, there was approximately a factor of 4 difference between the plain and the hybrid design. The leak rates for SS430 and mica in the hybrid design after 29 thermal cycles (∼0.012 sccm/cm) were approximately the same as the plain mica before the test (∼0.011 sccm/cm). This suggests that the leak is still predominately from the interfaces; however, it is between the bonded (to metal) mica sublayers and the adjacent mica sublayers (as shown schematically in Fig. 5-B) rather than through the mica itself, which is typically about $2-6 \times 10^{-4}$ sccm/cm under a stress of 100 psi. From optical microscopy, no spalling was observed along the glass-metal interface and the interlayer glass was strongly bonded to the metal along with one to two sub-layers of mica (the Muscovite single crystal mica sheet will cleave along the basal plane into sub-layers after losing the chemical waters at elevated temperatures [9]). It is clear

that the hybrid design gave better performance than the plain design in that the normalized leak rates for the hybrid design were approximately one-third of the rates for the plain design.

3.4. Multilayer thermal cycling of hybrid micas with SS430 and SS304 spacers

Planar SOFC stacks are fabricated by ''stacking'' multiple cells and interconnects in series. To investigate the effect of thermal cycling on the leak rates in stacks, multilayer test assemblies were prepared consisting of six layers of mica, five layers of either SS430 or SS304 spacers, and 12 layers of glass (Fig. 2). SS304 is known to be unsuitable for elevated temperature (∼800 °C) applications due to its poor oxidation resistance. However, it was chosen due to the similarity of its CTE (∼19 ppm/°C) to Inconel #600, and the unavailability of Inconel #600 in thin sheet. The normalized 800 °C leak rates for the multilayer hybrid seal tests are listed in Table 2, and plotted in Fig. 6. As observed in the single layer tests, the leak rates increased rapidly in the initial couple of cycles and then tended to flatten out. However, the initial normalized leak rates for multilayer seals (∼$5-9 \times 10^{-3}$ sccm/cm) were an order of magnitude
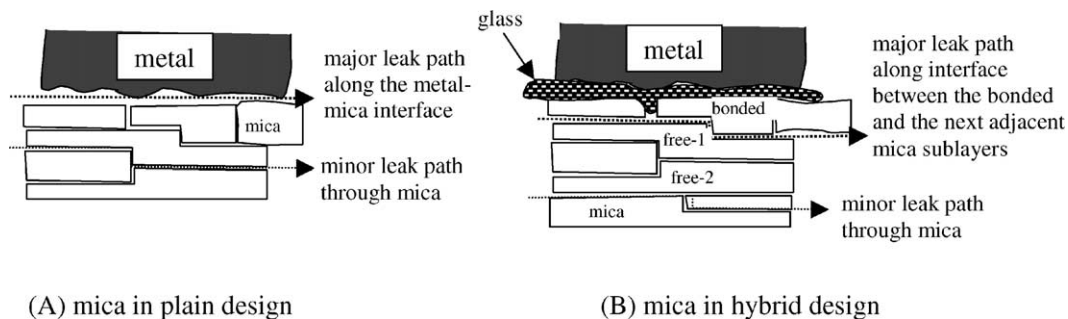

Fig. 5. Schematic drawing shows the major and minor leak path after thermal cycle test for the Muscovite single crystal mica in the plain (A) and hybrid design (B). Note that the single crystal Mica sheet cleaved into sub-layers (bonded, free-1, free-2, etc.) after losing chemical water.

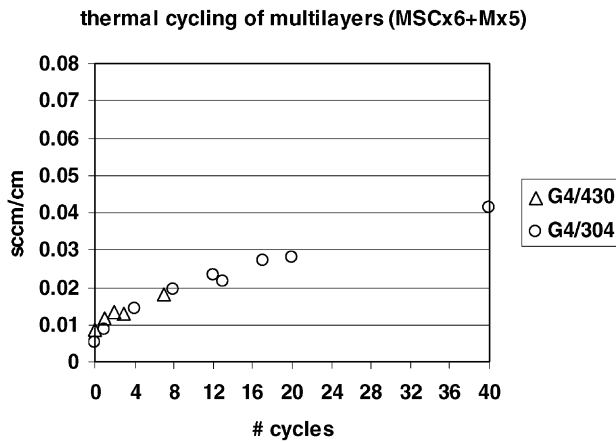**thermal cycling of multilayers (MSCx6+Mx5)**

Fig. 6. Normalized leak rates of multi-layer assembly with hybrid mica seals and two different metal spacers (SS304 or SS430) during thermal cycling at 800 °C and a compressive load of 50 lbs.

higher than that of the single layer seal tests ($\sim 2-6 \times 10^{-4}$ sccm/cm), and the leak rates after ~ 40 cycles were about three times larger than the single layer tests (Tables 1 and 2). One reason for the discrepancy was the fact that the actual compressive stress (nominally 100 psi) was likely dissipated through the six layers of mica and five layers of

stainless steel spacers since wider spacers were used (for easy alignment) for the test. From the impression on the pressed spacers at the bottom of the assembly (close to the alumina substrate), the applied stress at the bottom was estimated to be only approximately one-half of the stress at the top (close to the metal pipe). Nevertheless, the similar trend in leak rates versus thermal cycles suggests that the damage or wear mechanism is similar for multilayer assemblies; the materials degradation causing the increase in leak rates is discussed in the next section.

3.5. Materials degradation

3.5.1. Plain mica design

After thermal cycling, the Muscovite single crystal mica sheets in the plain design could be easily detached from the Inconel #600 loading pipe and the alumina substrate. No obvious damage to mica was observed and no chemical bonding was found between mica and the contacting materials. This implies good chemical stability of the mica at elevated temperatures and under stress for SOFC applications, although the stability in humid and reducing environments remains to be determined. However, distinct damage was revealed when examining the mica with optical microscopy. Fig. 7 shows the surface morphology of the
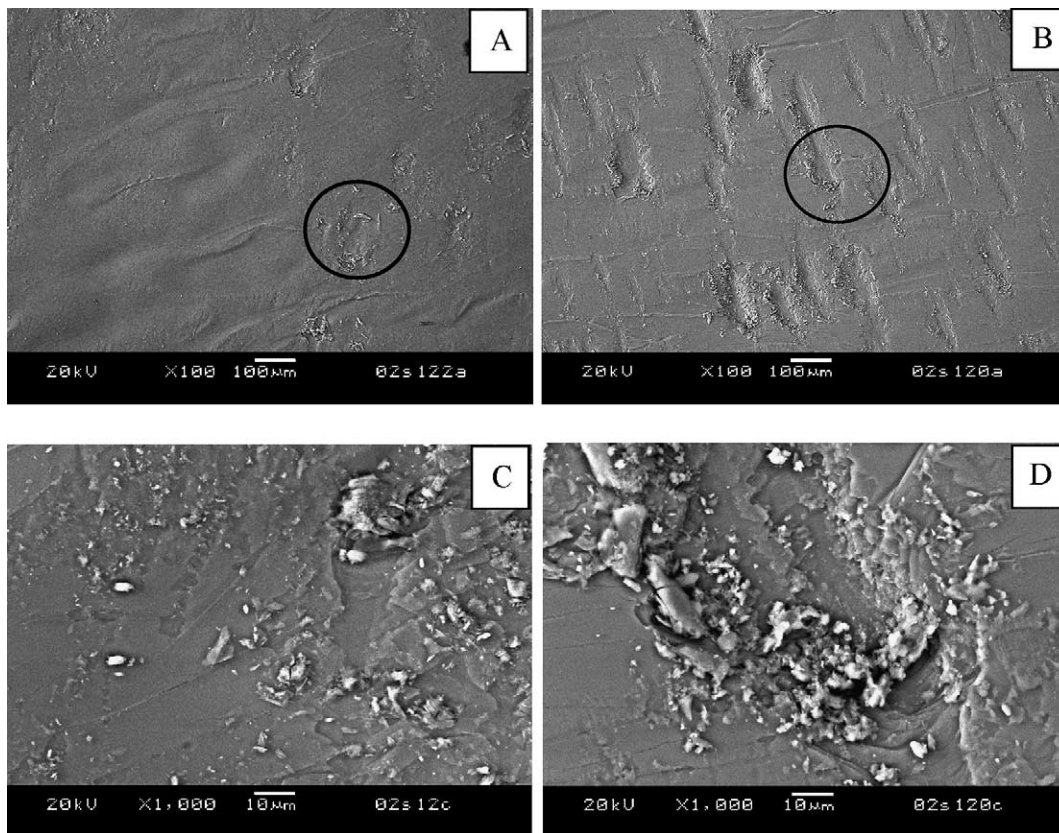

Fig. 7. Surface morphologies of the Muscovite single crystal mica in contact with the Inconel #600 pipe (without the glass interlayers) after (A) one thermal and (B) 24 thermal cycles at 800 °C and 100 psi in air: (C) and (D) are higher magnifications of the circled area in (A) and (B), respectively. The micrographs clearly show the degradation of mica at the circumference of the indentations.
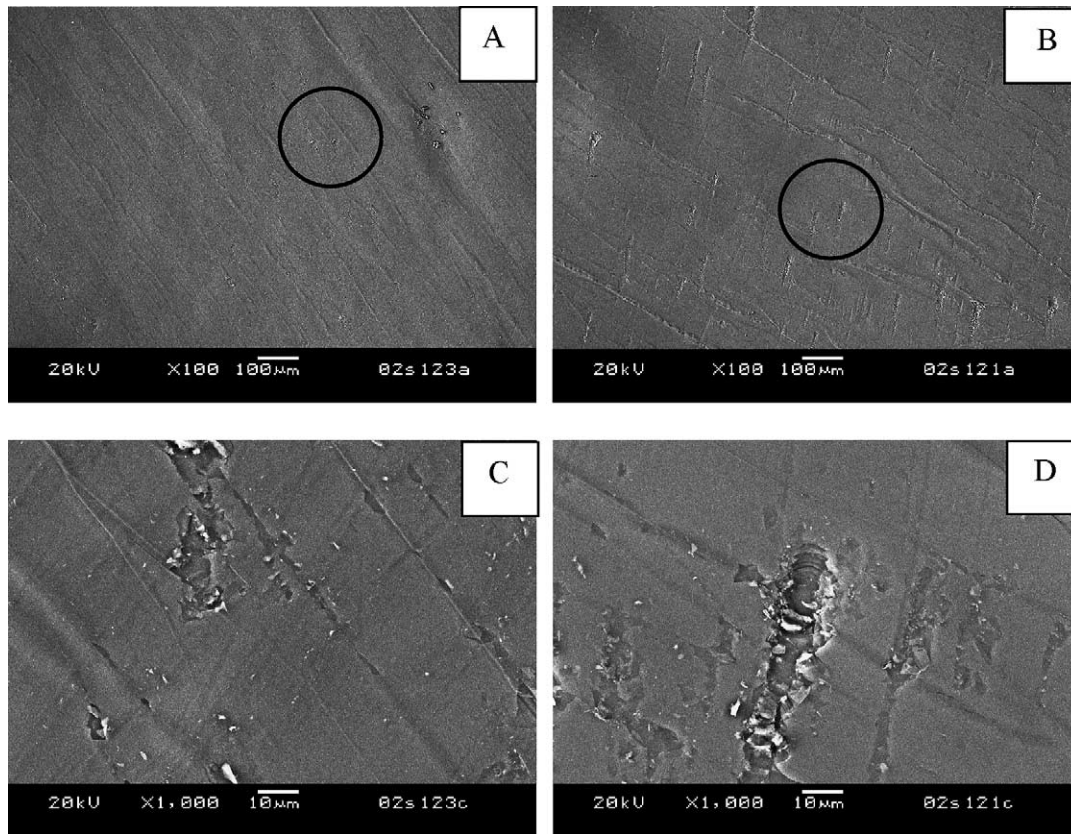
Fig. 8. Surface morphologies of the Muscovite single crystal mica in contact with the alumina substrate (without the glass interlayers) after (A) one thermal and (B) 24 thermal cycles at 800 °C and 100 psi in air: (C) and (D) are higher magnifications of the circled area in (A) and (B), respectively. The micrographs clearly show less degradation as compared to the surface in contact with Inconel #600.

Muscovite mica which had been in contact with the Inconel #600 loading pipe. Fig. 8 shows the surface which was in contact with the alumina substrate. There appeared to be two types of damage: indentations, and fragmentations around the circumference of the indentations. The cause for these indentations is attributed to the roughness of the contact surfaces, and it is apparent that the smoother alumina substrate resulted in smaller and shallower indentations than the Inconel #600 pipe (Figs. 7B and 8B). The fragmentations or particles around the circumferences were similar to the wear debris (particles) often observed in the sliding wear of ceramics [13], and can be attributed to the residual stresses (from CTE mismatch) at indentationss where the mica was mechanically interlocked with the mating surfaces. As a result, the damage appeared to be localized around the circumference (Fig. 7B). It is interesting to note that the fragmentations at the alumina side (Fig. 8D) were much less severe than at the metal side (Fig. 7D). This is probably due to the better CTE match at the alumina side than the metal side. To a first approximation, the residual stresses ($\Delta\alpha\Delta TE$) could be as high as 1.2 GPa ($\Delta\alpha = 12$ ppm/°C, $\Delta T = 700$ °C, E (Young's modulus) = 140 GPa) in compression in the micas at the metal side (and ∼0.2 GPa at the alumina side); the observed micro-fractures are likely due to a result of tensile and/or shear stress components due to surface asperities.

3.5.2. Hybrid mica design

There is a concern that the use of a low melting glasses as the seal interlayer could damage the materials in contact (e.g. metal, ceramic, and the mica itself), especially under the compressive stresses at elevated temperatures. After the cycling test, no degradation of the mica sheet was observed, except that several sub-layers of mica were bonded to the loading pipe and to the alumina substrate. The mica sheet could still be easily detached from the loading pipe and the alumina substrate. Fig. 9 shows the surface morphology of the mica (representing the "free-1" layer shown schematically in Fig. 5B). Clearly, there are steps (arrows in Fig. 9A) indicating the out-of-plane cleavage of Muscovite single crystal sheet. These steps are believed to cause the rapid increase in leak rates during the initial couple of thermal cycles (Fig. 4). Upon cooling, the "bonded" and "free-1" sub-layers experienced different thermal contractions (i.e. the bonded layer would be expected to behave similar to the metal since its thickness is insignificant compared to the metal) which led to the fracture or the micro-fracture. It is also interesting to note that the thermal cycle damage was rather limited as shown in Fig. 9B, i.e. it is localized only on the first contacting layer ("free-1" sub-layer). The layers underneath (e.g. "free-2" sub-layer in Fig. 5B) were found to be smooth and free from damage when a small section of
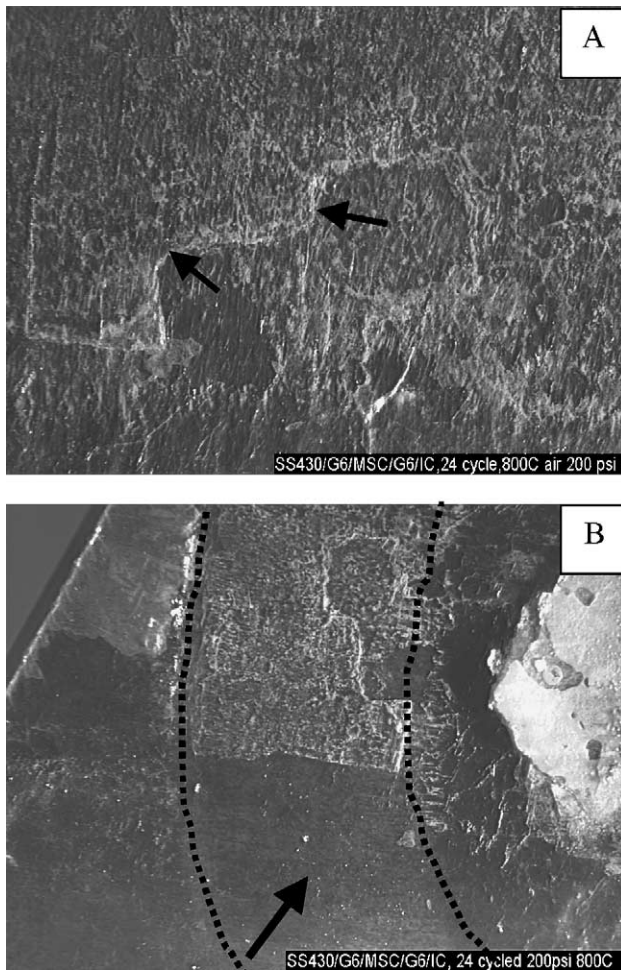
Fig. 9. Surface morphology of mica in the hybrid design after 24 thermal cycles at 800 °C showing (A) the steps (arrows) indicating the out of plane cleavage, and (B) the much smoother surface (arrow) indicating that the damage is limited only to the contact sub-layer (in the arrow region the contact sub-layer was deliberately peeled off to reveal the sub-layer underneath, and the dotted lines show the two boundaries of the pressed region).
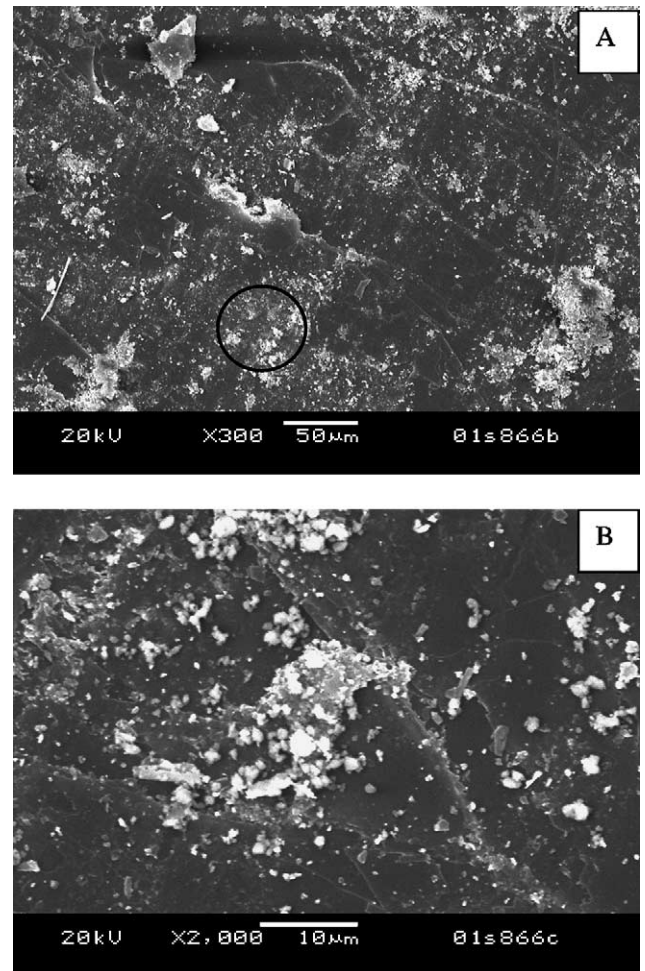

Fig. 10. Surface morphologies of the Muscovite single crystal mica after 21 thermal cycles at 800 °C and 100 psi in air in the hybrid seal design with the glass interlayers: (A) a low magnification, and (B) a high magnification of the circled area in (A).

the first contact layer was peeled off (arrow in Fig. 9B). Under higher magnification, the thermal cycle damage to mica in the hybrid design appeared to be more uniformly distributed, as no distinct indentations were observed as compared to the plain design. In addition, the fragments or particles were finer for the micas in the hybrid design (Fig. 10).

It is interesting to note that the thermal cycling damage to the compressive seal in terms of the leak rates are analogous to the sliding wear in ceramics. For example, the wear volume versus number of wear cycles of a SiC–TiB$_2$ particulate composite plate sliding by a SiC pin in a reciprocating sliding showed a similar behavior in terms of leak rate versus thermal cycles, i.e. a rapid initial increase followed by a gradual flattening out to a constant linear increase [13]. The wear mechanism was attributed to the failure of the particle–matrix interface, resulting in the particle pullout

and chipping of the matrix. The generated wear debris was often "recycled" through the contact interfaces, resulting in the production of sub-micrometer particles. The authors suggested lowering the interfacial friction rather than increasing the fracture toughness as the primary guidelines for designing ceramic composites for tribological applications. It is not clear whether that guideline can be applied to the present application. For compressive micas, the friction of mica against mica would probably be small since they cleaved on parallel basal planes. Consequently, one would like to have a stronger or tougher mica to withstand the thermal cycle damages.

3.6. Applications to SOFC

Low fuel leak rates are required if SOFC stacks are to operate safely and economically. Although the allowable leak rates remain to be determined and will be somewhat design-specific, common sense points to the use of sealing materials offering leak rates as low as possible at a compressive stress as

low as possible. The hybrid seal based on the Muscovite single crystal mica appears to be a viable candidate, considering the low leak rates reported above. For a 60-cell (14 cm × 14 cm per cell) stack of 4 kW, 65% fuel utilization, 20% oxygen utilization, 0.5 W/cm^2, the total fuel flow rate is estimated to be ∼2.18 × 10^5 sccm (STP) [11]. Assuming that the leak rate measured in this study (0.0119 sccm/cm, Table 1, hybrid design after 29 cycles) applied to full size stacks, the total leak rate for a 60-cell stack at 800 °C after 1300 thermal cycles (equivalent to 5-year heavy-duty truck operation at 1 cycle per day and 260 days per year) would be only ∼0.9% of the total fuel rate for the hybrid Muscovite single crystal mica seal under an applied compressive stress of 100 psi and a 2 psi pressure gradient (a leak length of 124 cm was assumed for each layer). While this assumption is somewhat simplistic, the current results clearly demonstrate the potential applicability of the hybrid-type compressive mica seals to SOFC applications. It needs to be emphasized, however, that other important aspects, such as long-term stability in reducing and humid environments, must be evaluated. Results of studies in reducing environments will be presented in the near future.

4. Conclusions

Thermal cycling was conducted on compressive mica seals at 800 °C in air in both the plain and the hybrid design. The hybrid design involves adding two glass interlayers and was found to greatly reduce the leak rates. Two metals (Inconel #600 and SS430) with high and low coefficient of thermal expansion were used to evaluate the effect of CTE mismatch on thermal cycling. The results showed that the leak rates were lower for the hybrid design than the plain micas. In addition, use of the lower CTE (SS430) metal pipe resulted in lower leak rates as compared to Inconel #600 metal (with higher CTE). In general, the leak rates increased rapidly in the initial couple of thermal cycles and tended to level off after several tens of thermal cycles. Microstructural examination revealed indents, steps, fragmentation and particle formation on the mica surface after thermal cycling. The degradation of the mica is attributed to residual stresses at contact asperities and cleavage steps due to CTE mismatch between mica and metals. Assuming a linear scale-up, the Muscovite mica in the hybrid design would yield a fuel leak of ∼0.9% of the total fuels for a 60-cell stack.

References

[1] N.Q. Minh, Ceramic fuel cells, J. Am. Ceram. Soc. 76 (3) (1993) 563–588.

[2] S.C. Singhal, Progress in tubular solid oxide fuel cell technology, in: S.C. Singhal, M. Dokiya (Eds.), Solid Oxide Fuel Cells (SOFC VI) Proceedings of the Sixth International Symposium, The Electrochemical Society, Honolulu, Hawaii, vol. 99-19, 1999, pp. 39–51.

[3] R. Bolden, K. Foger, T. Pham, Towards the development of a 25 kW planar SOFC system, in: S.C. Singhal, M. Dokiya (Eds.), Solid Oxide Fuel Cells (SOFC VI) Proceedings of the Sixth International Symposium, The Electrochemical Society, Honolulu, Hawaii, vol. 99-19 (1999) 80–87.

[4] A. Khandkar, S. Elangovan, J. Hartvigsen, D. Rowley, R. Privette, M. Tharp, Status and progress in SOFCo's planar SOFC development, in: S.C. Singhal, M. Dokiya (Eds.), Solid Oxide Fuel Cells (SOFC VI) Proceedings of the Sixth International Symposium, The Electrochemical Society, Honolulu, Hawaii, vol. 99-19, 1999, pp. 88–94.

[5] N. Lahl, L. Singheiser, K. Hilpert, K. Singh, D. Bahadur, Aluminosilicate glass ceramics as sealant in SOFC stacks, in: S.C. Singhal, M. Dokiya (Eds.), Solid Oxide Fuel Cells (SOFC VI) Proceedings of the Sixth International Symposium, The Electrochemical Society, Honolulu, Hawaii, vol. 99-19, 1999, pp. 1057–1065.

[6] T. Yamamoto, H. Itoh, M. Mori, N. Mori, T. Watanabe, Compatibility of mica glass–ceramics as gas-sealing materials for SOFC, Denki Kagaku 64 (6) (1996) 575–581.

[7] K. Ley, M. Krumpelt, J. Meiser, I. Bloom, J. Mater. Res. 11 (1996) 1489.

[8] P. Larsen, C. Bagger, M. Morgensen, J. Larsen, in: M. Dokiya, O. Yamamoto, H. Tagawa, S. Singhal (Eds.), Solid Oxide Fuel Cells. IV, vol. 69, PV 95-1, The Electrochemical Society, Pennington, NJ, 1995.

[9] S.P. Simner, J.W. Stevenson, Compressive mica seals for SOFC applications, J. Power Sources 102 (1-2) (2001) 310–316.

[10] N. Lahl, D. Bahadur, K. Singh, L. Singheiser, K. Hilpert, J. Electrochem. Soc. 149 (5) (2002) A607–A614.

[11] Y.-S. Chou, J.W. Stevenson, L.A. Chick, J. Power Sources, submitted for publication.

[12] G. Hishmeh, L. Gartz, F.G. Karioris, C. Templier, J. Chaumont, C. Clerc, J. Am. Ceram. Soc. 76 (2) (1993) 343–346.

[13] O.O. Ajayi, A. Erdemir, R.H. Lee, F.A. Nichols, J. Am. Ceram. Soc. 76 (2) (1993) 511–517.